International Journal of GEOMATE, Jan., 2026 Vol.30, Issue 137, pp.131-138
ISSN: 2186-2982 (P), 2186-2990 (O), Japan, DOI: https://doi.org/10.21660/2026.137.g15307
Geotechnique, Construction Materials and Environment

CORRELATION BETWEEN INFILL DENSITY AND MECHANICAL PROPERTIES IN 3D PRINTING

*Boonthum Wongchai, and Suphattharachai Chomphan

Faculty of Engineering at Sriracha, Kasetsart University, Thailand

*Corresponding Author, Received: 27 May 2025, Revised: 16 Dec. 2025, Accepted: 20 Dec. 2025

ABSTRACT: Fused Deposition Modeling (FDM) has emerged as a transformative technology in additive manufacturing, yet the precise influence of infill density on the mechanical behavior of toughened filaments, such as enhanced polylactic acid (PLA+), remains insufficiently characterized. This study systematically investigates the correlation between infill density and the mechanical properties of PLA+ specimens fabricated using a consistent grid infill pattern. To ensure a comprehensive analysis, specimens were printed with infill densities ranging from 20% to 100% at fine 10% intervals, strictly adhering to ASTM D638-14 testing standards. Statistical regression analysis revealed that both Young's modulus and yield strength exhibit strong positive linear relationships with infill density ($R^2 \geq 0.98$), indicating a direct proportionality between material volume and stiffness. The ultimate tensile strength was best modeled by a quadratic equation ($R^2 = 0.98$). A pivotal finding of this research is the behavior of the strength-to-weight ratio, which exhibited a non-monotonic, U-shaped characteristic ($R^2 = 0.71$) rather than a linear progression. The analysis identified optimal material efficiency at low densities (20–30%) and near-solid densities (90–100%), whereas the mid-range (40–80%) displayed diminishing returns where weight accumulation outpaced strength gains. These findings provide critical guidelines for civil and geotechnical engineering applications, such as the design of lightweight concrete formworks and scaled physical models. The derived empirical models enable engineers to predict performance and optimize printing parameters, effectively balancing structural integrity with material sustainability and cost-efficiency.

Keywords: Infill density, 3-D printing, Enhanced Polylactic Acid (PLA+), Mechanical Properties

1. INTRODUCTION

In recent years, 3D printing has emerged as a key technology within the field of additive manufacturing (AM), offering the ability to fabricate complex geometries with minimal material waste and shorter production times compared to conventional methods. The AM process typically begins with a CAD-designed prototype exported as an STL file, which is then processed by slicing software to generate G-code for layer-by-layer fabrication. This layer-wise manufacturing approach allows precise control over internal architecture and material distribution. AM supports a wide range of materials, including polymers, metals, ceramics, and composite blends, making it suitable for applications across aerospace, automotive, robotics, and sensor technologies. Among various AM technologies such as stereolithography (SLA) and multi jet fusion (MJF), fused deposition modeling (FDM) is the most widely adopted due to its low cost, ease of use, and material versatility [1–3].

Beyond industrial applications, FDM 3D printing has gained interest in construction and geotechnical engineering. PLA-based materials, including enhanced PLA+ filaments, are being explored for temporary or lightweight structural elements such as formwork, soil-retaining structures, erosion control modules, and physical modeling in geotechnical testing. Their biodegradability and ease of fabrication make them appealing for sustainable and low-impact environmental applications. Understanding how infill density influences the mechanical properties of these printed materials is therefore essential for optimizing performance and safety in such engineering contexts, particularly where weight reduction and material efficiency are critical design constraints.

In 3D printing, materials are selected based on desired properties such as strength and application requirements. PLA (Polylactic Acid) is widely used due to its ease of use, low printing temperature, and biodegradable nature. PLA+ is an enhanced version of PLA that includes additives to improve strength, durability, and surface finish. ABS offers improved toughness and temperature resistance but requires controlled printing conditions, while PETG combines ease of printing with enhanced durability and chemical resistance.

To further improve mechanical capabilities, recent studies have focused on advanced material modifications. Composite materials, such as PLA reinforced with recycled desized carbon fiber shells, significantly enhance tensile modulus and strength by restricting polymer chain mobility [4]. Polymer blends such as PLA/TPU improve ductility but often reduce stiffness due to the elastic nature of TPU [5]. Sandwich printing techniques, including PLA/wood composites and carbon fiber–reinforced PLA systems, are increasingly used to balance weight reduction and structural integrity [6, 7].

Printing parameters—including infill pattern, infill density (ID), build orientation, raster angle, nozzle temperature, bed temperature, extrusion speed, and nozzle diameter—significantly affect mechanical properties such as Young's modulus, yield strength, and ultimate strength [8–12]. For PLA, increasing infill density enhances stiffness and strength [13, 14]. In contrast, while high-performance polymers such as PEEK depend strongly on thermal management and post-processing [15], for engineering thermoplastics like PLA+, structural geometry—particularly infill density—plays a more dominant role. Apart from material selection, the infill pattern is a critical determinant of structural stability. In this study, a grid pattern was selected due to its geometric stability and load-bearing capability. However, unlike standard PLA, increasing infill density in PLA+ not only increases material volume but also affects inter-layer bonding and thermal accumulation during printing, indicating that mechanical responses may not be strictly linear.

Although extensive research has been conducted on PLA and other polymers, studies specifically investigating the effect of infill density on the mechanical properties of PLA+ remain limited. This creates a knowledge gap regarding whether the toughened nature of PLA+ alters stress distribution mechanisms compared to brittle PLA. To address this gap, the present study employs PLA+ filament to evaluate the mechanical performance of 3D-printed specimens fabricated with varying infill densities using a consistent grid pattern. The influence of infill density on tensile strength and stiffness is systematically examined, and statistical regression analysis is used to quantify the correlation between infill density and mechanical properties. The subsequent sections present a systematic evaluation of the mechanical behavior of PLA+ as a function of infill density, examine the relationship between infill density and Young's modulus, and analyze yield strength and ultimate tensile strength using both linear and quadratic regression models.

2. RESEARCH SIGNIFICANCE

The primary novelty of this study lies in its high-resolution, density-dependent evaluation of PLA+ mechanical behavior under a fixed and structurally stable grid infill configuration. Unlike prior studies that rely on coarse density intervals or focus on conventional PLA, this research captures fine mechanical transitions by incrementally varying infill density at 10% steps from 20% to full solidity. This approach enables the derivation of statistically robust empirical relationships that distinguish linear stiffness evolution from nonlinear strength responses. The identification of quadratic behavior in ultimate tensile strength highlights material–structure interactions unique to toughened PLA+, which are not evident in brittle polymer systems.

3. MATERIALS AND METHODS

According to ASTM D638-14, the standard test method for tensile properties of plastics, a Type I specimen with a thickness of 3.2 mm is designed using SOLIDWORKS software (Fig.1) and exported as an STL file [16]. Creality Slicer software is used to generate the G-code files by varying the infill density at 20%, 30%, 40%, 50%, 60%, 70%, 80%, 90%, and 100%. A grid infill pattern with a raster angle of 45° is applied (Fig.2). All specimens are fabricated using a Creality CR-10 Smart 3D printer with eSUN PLA+ filament, which has a density of 1.23 g/cm³.

The nozzle diameter used in the printing process was 0.4 mm, and the layer height was maintained at 0.2 mm to ensure dimensional accuracy. The top and bottom layer thicknesses were set to 0.4 mm, with four layers applied for both the top and bottom surfaces, using 100% infill in these regions to provide solid shell layers. The nozzle temperature was set at 200 °C, and the heated bed temperature was maintained at 60 °C to enhance adhesion during printing. A print speed of 50 mm/s was selected to balance print quality and production time. Each specimen was printed in a horizontal orientation on the build plate to minimize warping and ensure flatness. After printing, specimens were conditioned at room temperature for 24 hours prior to mechanical testing. These printing parameters were selected based on standard practices and prior research that demonstrated their effectiveness in producing dimensionally accurate and mechanically consistent PLA-based parts [17].

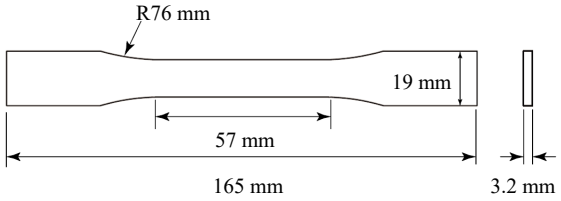

Fig.1 ASTM D638-14 specimen dimension.

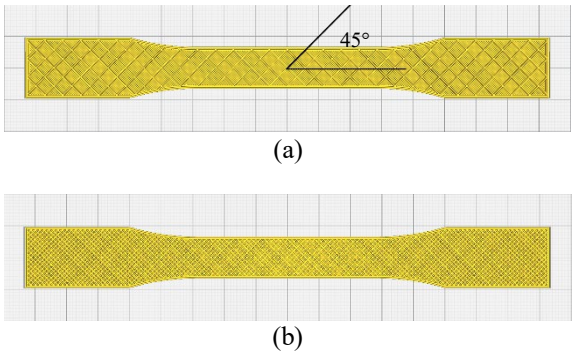

Fig.2 Infill density settings in Creality Slicer

software: (a) 20% infill, (b) 80% infill.

Three specimens for each infill density are tested using an Instron 5982 universal testing machine, equipped with a 100 kN load cell and operated at a crosshead speed of 5 mm/min, as shown in Fig.3. Prior to tensile testing, each specimen was weighed using a precision analytical balance (Shimadzu AY220, Shimadzu Corporation, Japan) with a maximum capacity of 220 g and a readability of 0.0001 g (0.1 mg) to ensure accurate mass measurement. The test is conducted using Bluehill software to control and monitor the testing process. Stress-strain curves are generated for each test, as illustrated in Fig.4. The Mechanical properties evaluated include Young's modulus (E), yield strength (σ_Y) determined using a 0.2% offset, ultimate tensile strength (σ_U), strength-to-weight ratio (α), tensile strength at break (σ_B), and tensile strain at break (ε_B). These parameters provide a comprehensive understanding of the material's tensile behavior under varying internal structures. The results are used to assess the influence of infill density on the overall mechanical performance of the printed specimens.

(a) (b)

Fig.3 (a) Tensile testing setup, and (b) fractured specimens after testing.

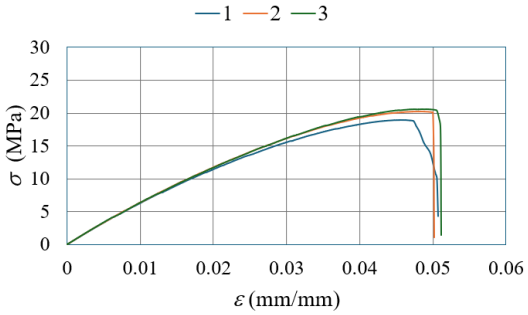

Fig.4 Stress-strain curve at 30% infill.

Regression analysis is used to describe the relationship between mechanical properties and infill density. This relationship can be represented by a polynomial equation as follows:

$$y = a_n ID^n + a_{n-1} ID^{n-1} + \ldots + a_2 ID^2 + a_1 ID + a_0, \quad (1)$$

where y is the dependent mechanical property, ID is the infill density, a_n are the polynomial coefficients, and n is the degree of the polynomial (e.g., n = 1 for linear, n = 2 for quadratic, n = 3 for cubic, etc.). The R^2 value, or coefficient of determination, indicates how well the regression model fits the data. An R^2 close to 1.0 means the model explains nearly all the variability of the response variable, suggesting a strong correlation. For example, an R^2 of 0.99 implies that 99% of the variation is accounted for by the model, indicating high predictive accuracy. Discussing R^2 values helps readers assess the reliability of the relationship and the strength of the predictor variable in each graph.

4. RESULTS AND DISCUSSION

3.1 Young's Modulus

Fig.5 presents the plot of Young's modulus versus infill density. The results indicate a linear relationship between Young's modulus and infill density. Through regression analysis, this relationship can be expressed as:

$$E = 4.0151\ ID + 346.58 \quad (2)$$

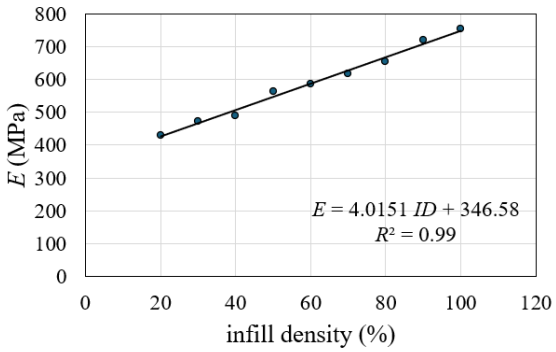

Fig.5 Young's modulus vs infill density with n = 1.

Eq. (2) has an R^2 value of 0.99, indicating a high degree of accuracy. This suggests that infill density is a strong predictor of the material's stiffness. Therefore, by adjusting the infill density, the mechanical properties of the printed part can be effectively tailored.

3.2 Yield Strength

Similar to the plot of Young's modulus versus infill density, the relationship between yield stress and infill density also exhibits a linear trend, as shown in Fig.6. The regression analysis reveals a strong linear correlation with a high R^2 value of 0.98, indicating excellent accuracy. This relationship can be expressed as:

$$\sigma_Y = 0.091\ ID + 14.793 \quad (3)$$

This result suggests that infill density is a strong predictor of the material's yield strength, allowing for precise control of mechanical properties through infill adjustments. Such control is critical for designing parts that meet specific strength requirements without unnecessary material use.

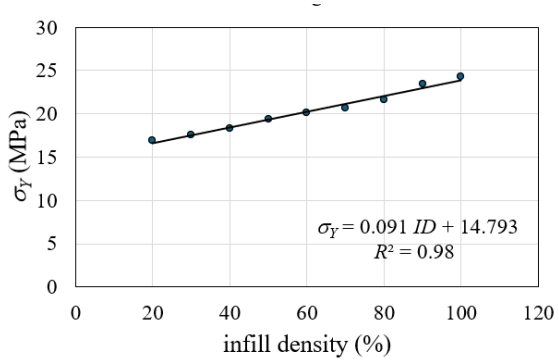

Fig.6 Yield strength vs infill density with n = 1.

3.3 Ultimate Tensile Strength

For ultimate tensile strength, a linear regression can be plotted with an R^2 value of 0.9218, as shown in Fig.7. The relationship between ultimate tensile strength and infill density can initially be expressed as:

$$\sigma_U = 0.1264\ ID + 15.608 \quad (4)$$

Although Eq. (4) demonstrates a reasonably strong correlation, the stress-strain curve at 30% infill in Fig.4 and similarly at other infill levels reveals a nonlinear behavior in the plastic deformation region. This suggests that a nonlinear model may better represent the relationship. Consequently, a quadratic regression with n = 2 was applied, also shown in Fig.8, resulting in an improved fit with an R^2 value of 0.98:

$$\sigma_U = 0.0014\ ID^2 - 0.044\ ID + 19.774 \quad (5)$$

This result confirms that infill density is a strong predictor of the material's ultimate tensile strength, and that quadratic regression provides a more accurate model for capturing the mechanical behavior, particularly in the plastic region.

The nonlinear model was found to better represent the relationship between infill density and ultimate tensile strength, as indicated by the improved R^2 value of 0.98 compared to the linear model. This is consistent with the behavior observed in the stress–strain curves (e.g., Fig. 4), where the material exhibits nonlinear plastic deformation, especially at lower infill densities. Linear models tend to oversimplify this behavior by failing to account for the gradual transition from elastic to plastic deformation and the complex internal stress distribution in FDM-printed structures.

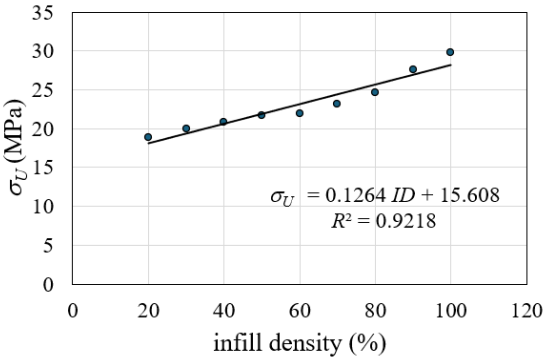

Fig.7 Ultimate tensile strength vs infill density with n = 1.

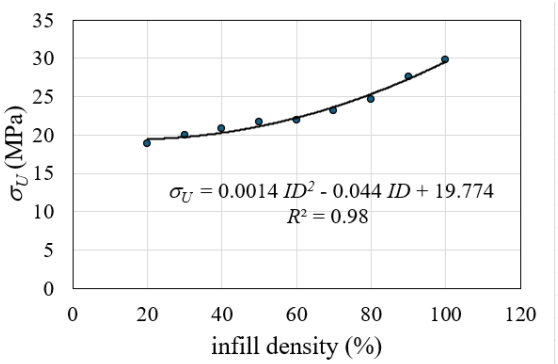

Fig.8 Ultimate tensile strength vs infill density with n = 2.

Previous studies have also reported similar findings. The mechanical properties of FDM-printed components are influenced by a combination of process parameters, such as infill density, due to factors like layer adhesion, void content, and anisotropic material behavior, all of which contribute to nonlinear performance trends. The ultimate tensile strength does not increase linearly with infill density, owing to the irregular stress distribution and fracture mechanisms introduced by internal porosity and layer geometry [18, 19]. These insights support the use of a quadratic model, which more accurately captures the mechanical response of printed specimens across different infill levels.

3.4 Strength-to-Weight Ratio

As illustrated in Fig. 9, the relationship between infill density and specific strength does not follow a simple linear trend but rather exhibits a non-monotonic, U-shaped behavior. The data were fitted with a quadratic regression model, revealing distinct efficiency zones:

$$\alpha = 0.0002\ ID^2 - 0.0224\ ID + 3.6938 \quad (6)$$

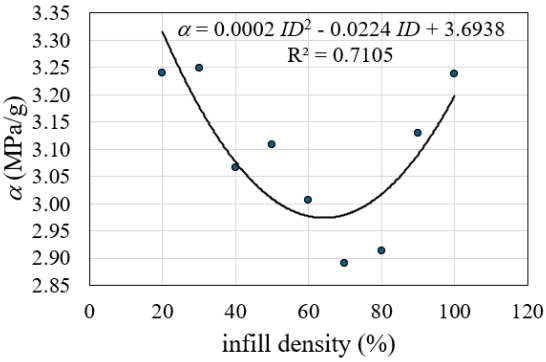

Fig.9 Strength-to-weight ratio vs infill density with n = 2.

The analysis indicates that material efficiency is optimized at the two extremes of the density spectrum.

Low-Density Efficiency (20-30%): The highest initial ratios (≈ 3.25 MPa/g) were observed in this range. At these densities, the grid structure effectively maintains geometric stability while minimizing mass.

Mid-Range Fluctuation (40-80%): As the density increases, the ratio declines to a minimum of approximately 2.89 MPa/g at 70% infill. The correlation coefficient (R^2 = 0.7105) reflects the inherent variability in this transition zone, where the interplay between infill geometry and bonding quality causes minor fluctuations in structural efficiency. High-Density Recovery (90-100%): Beyond 80%, the ratio recovers significantly, reaching 3.24 MPa/g at 100% density, suggesting that the reduction of voids in solid-like structures compensates for the added weight.

3.5 Tensile Strength at Break

Fig.10 presents the plot of tensile strength at break versus infill density. A quadratic regression provides the fit for the data, with an R^2 value of 0.6737, and can be expressed as:

$$\sigma_B = 0.0006\ ID^2 + 0.0664\ ID + 13.079 \quad (7)$$

Understanding tensile strength and strain at break is essential for assessing the mechanical performance and failure resistance of 3D-printed parts. These properties indicate how much stress and deformation a material can withstand before breaking, which is critical for load-bearing applications or safety-critical components.

The relatively low R^2 value (67.37%) reflects the variability and complexity of fracture behavior during tensile testing. The apparent scattering of data points in Fig.10 may partially result from human factors such as inconsistencies in specimen preparation, printing parameters, or testing alignment. To overcome these issues, more rigorous control of experimental conditions is recommended such as using automated calibration of tensile test machines, maintaining uniform environmental conditions (e.g., temperature and humidity), and increasing the number of replicates to minimize outlier influence and improve statistical reliability.

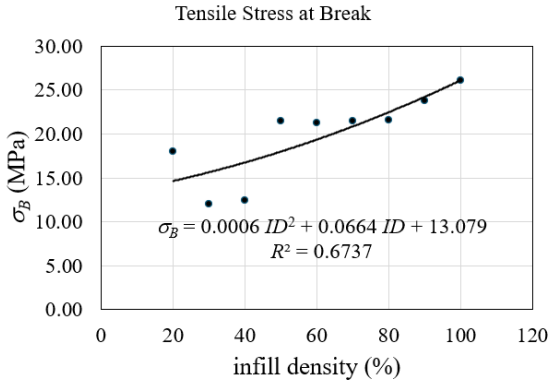

Fig.10 Tensile strength at break vs infill density with n = 2.

3.6 Tensile Strain at Break

Similar to the tensile strength at break, the relationship between infill density and tensile strain at break is best represented by a quadratic regression, as shown in Fig.11. The equation is expressed as:

$$\varepsilon_B = 9\times10^{-6}\ ID^2 - 0.0012\ ID + 0.0833 \quad (8)$$

This model yields an R^2 value of 0.7795, indicating an accuracy of 77.95% in predicting the strain at break. The relatively moderate accuracy is attributed to the complex and inconsistent nature of fracture behavior during tensile testing.

As shown in Fig. 11, the tensile strain at break initially decreases with increasing infill density up to approximately 60%, after which it begins to increase. This trend can be explained by the interplay between structural stiffness and material deformability. At lower infill densities, the internal structure is more compliant, allowing greater elongation before failure. As the infill density increases, the structure becomes stiffer and more constrained, reducing the strain at break. However, beyond 60%, the higher material continuity and internal support may enhance energy dissipation and delay crack propagation, leading to an increase in tensile strain at break. Consequently, the mechanical behavior at high densities transitions towards that of a solid material, allowing the inherent ductility of the PLA+ filament to fully manifest.

Although increasing the polynomial degree to n = 6 improves the R^2 value to above 0.95 for both tensile strength and tensile strain at break, such high-degree polynomial models tend to overfit the data. While they may fit the experimental points closely, they lack physical interpretability and are not suitable for reliably predicting real-world mechanical behavior.

Table 1. Summary of regression models and correlation coefficients (R^2) for mechanical properties of PLA+ at different infill densities.

Mechanical Property	Regression Equation	R^2 Value	Relationship Type
Young's Modulus	$E = 4.0151\ ID + 346.58$	0.99	Linear
Yield Strength	$\sigma_Y = 0.091\ ID + 14.793$	0.98	Linear
Ultimate Tensile Strength	$\sigma_U = 0.0014\ ID^2 - 0.044\ ID + 19.774$	0.98	Quadratic
Strength-to-Weight Ratio	$\alpha = 0.0002\ ID^2 - 0.0224\ ID + 3.6938$	0.7105	Quadratic
Tensile Strength at Break	$\sigma_B = 0.0006\ ID^2 + 0.0664\ ID + 13.079$	0.6737	Quadratic
Tensile Strain at Break	$\varepsilon_B = 9\times10^{-6}\ ID^2 - 0.0012\ ID + 0.0833$	0.7795	Quadratic

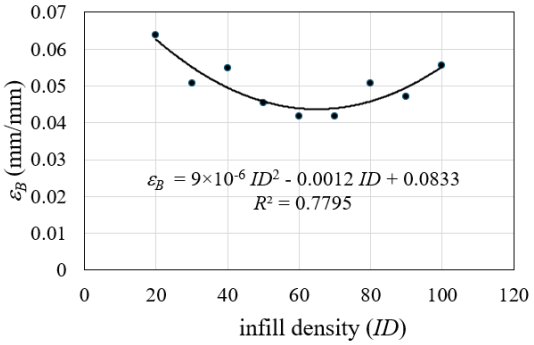

Fig.11 Tensile strain at break vs infill density with $n = 2$.

3.7 Failure Mechanism

The failure mechanism is directly correlated with the infill density level:

Low Infill Density (20-40%): Failure typically initiates with the buckling of the internal grid structure before the outer shell tears. This behavior indicates that at lower densities, the specimen's

strength is predominantly governed by the structural stability of the infill rather than the material's intrinsic strength.

High Infill Density (60-100%): The specimens exhibit behavior closer to that of a bulk material. Failure occurs as a distinct trans-raster fracture, indicating a brittle failure mode. This aligns with the tensile test results, where the Ultimate Tensile Strength followed a quadratic relationship ($R^2 \approx 0.98$), suggesting that as the material density increases, load transmission becomes fully efficient up to the point of failure.

Table 1 summarizes the mathematical correlations derived from the experimental results. It presents the regression equations and the corresponding coefficient of determination (R^2) values for each mechanical property, providing a quantitative basis for predicting the material behavior of PLA+ at various infill densities. These empirical models facilitate the optimization of printing parameters, allowing engineers to estimate the expected tensile strength and stiffness without the need for extensive physical testing. Furthermore, they serve as essential inputs for computational simulations, such as Finite Element Analysis (FEA), enabling the accurate prediction of structural performance for complex geometries prior to fabrication.

5. POTENTIAL APPLICATIONS

The findings regarding the correlation between infill density and the mechanical properties of PLA+ have direct implications for civil and geotechnical engineering applications:

4.1 Lightweight Formwork Systems

For complex concrete casting, 3D-printed PLA+ formworks can be optimized by reducing the infill density to 50-60%. Results indicate that this density range maintains sufficient Yield Strength to withstand hydrostatic pressure from fresh concrete while significantly reducing the mold weight and material costs compared to solid printing.

4.2 Scaled Physical Modeling

In geotechnical physical modeling (e.g., slope stability or seismic simulations), researchers require materials with scaled-down stiffness (Young's Modulus). Using the linear regression model derived from this study ($E \approx 4.01 \times ID + \text{Constant}$), researchers can precisely select a specific Infill Density to match the required stiffness dictated by Similitude Laws, offering a flexible alternative to changing material types."

6. CONCLUSION

This study systematically investigated the influence of infill density (20% to 100%) on the mechanical performance and structural efficiency of enhanced PLA+ specimens fabricated via FDM using a grid pattern. Based on the experimental results and regression analysis, the following conclusions can be drawn:

1. Mechanical Correlations: The infill density serves as a critical determinant for mechanical properties. Young's modulus and yield strength exhibited a strong linear positive correlation with infill density ($R^2 \geq 0.96$), indicating that stiffness increases proportionally with material volume. The ultimate tensile strength was best described by a quadratic model ($R^2 \geq 0.98$), confirming predictable load-bearing improvements with increased density.

Conversely, tensile strain and strength at break showed weaker correlations ($R^2 < 0.9$), suggesting a higher sensitivity to print imperfections in the post-yield region.

2. Structural Efficiency (Strength-to-Weight Ratio): A distinct trade-off was observed in material efficiency. Unlike absolute strength, the strength-to-weight ratio followed a non-monotonic, U-shaped trend. Optimal specific strength was identified at low densities (20–30%), making them ideal for lightweight applications, and at near-solid densities (90–100%), where material continuity maximizes performance. Intermediate densities (40–80%) demonstrated diminished returns, where the increase in weight outpaced the gain in strength.

3. Implications: The derived regression models provide a practical framework for engineering design. These findings allow for the precise tailoring of PLA+ components enabling engineers to prioritize either weight reduction or maximum structural integrity depending on the specific requirements of geotechnical and construction applications.

7. ACKNOWLEDGMENTS

The author gratefully acknowledges the support of the Applied Mechanics and Product Design (AMPD) research group, Faculty of Engineering at Sriracha, Kasetsart University, Sriracha Campus. The resources and expertise provided by the group were instrumental in the successful completion of this work.

8. REFERENCES

1. Tran T. Q., Ng F. L., Tan J. T. Y. K., Feih S., and Nai M. L. S., Tensile Strength Enhancement of Fused Filament Fabrication Printed Parts: A Review of Process Improvement Approaches and Respective Impact. Additive Manufacturing, 54, 2022, Article 102724. https://doi.org/10.1016/j.addma.2022.102724
2. Kumar S., Singh H., Singh I., Bharti S., Kumar D., Siebert G., and Koloor S. S. R., A comprehensive review of FDM printing in sensor applications: Advancements and future perspectives. Journal of Manufacturing Processes, Vol. 113, 2024, pp. 152–170. https://doi.org/10.1016/j.jmapro.2024.01.030
3. Kadhum A. H., Al-Zubaidi S., and Abdulkareem S. S., Effect of the Infill Patterns on the Mechanical and Surface Characteristics of 3D Printing of PLA, PLA+ and PETG Materials. ChemEngineering, Vol. 7, 2023, Article 46. https://doi.org/10.3390/chemengineering7030046
4. Saleh M., Anwar S., AlFaify A. Y., Al-Ahmari A. M., and Abd Elgawad A. E. E., Development of PLA/recycled-desized carbon fiber composites for 3D printing: Thermal, mechanical, and morphological analyses. Journal of Materials Research and Technology, Vol. 29, 2024, pp. 2768–2780. https://doi.org/10.1016/j.jmrt.2024.01.267
5. Hamidi M. N., Abdullah J., Mahmud A. S., Hassan M. H., and Zainoddin A. Y., Influence of thermoplastic polyurethane (TPU) and printing parameters on the thermal and mechanical performance of polylactic acid (PLA)/thermoplastic polyurethane (TPU) polymer. Polymer Testing, Vol. 143, 2025, Article 108697. https://doi.org/10.1016/j.polymertesting.2025.108697
6. Kechagias J. D. and Zaoutsos S. P., An assessment of PLA/wood with PLA core sandwich multilayer component tensile strength under different 3D printing conditions. Journal of Manufacturing Processes, Vol. 131, 2024, pp. 1240–1249. https://doi.org/10.1016/j.jmapro.2024.09.098
7. Subramaniyan M., Karuppan S., Appusamy A., and Pitchandi N., Sandwich printing of PLA and carbon fiber reinforced-PLA for enhancing tensile and impact strength of additive manufactured parts. Journal of Manufacturing Processes, Vol. 137, 2025, pp. 425–436 https://doi.org/10.1016/j.jmapro.2025.02.001
8. Hikmat M., Rostam S., and Ahmed Y. M., Investigation of tensile property-based Taguchi method of PLA parts fabricated by FDM 3D printing technology. Results in Engineering, Vol. 11, 2021, Article 100264. https://doi.org/10.1016/j.rineng.2021.100264
9. Nyabadza A., Mc Donough L. M., Manikandan A., Basu Ray A., Plouze A., Muilwijk C., Freeland B., Vazquez M., and Brabazon D., Mechanical and antibacterial properties of FDM additively manufactured PLA parts. Results in Engineering, Vol. 21, 2024, Article 101744. https://doi.org/10.1016/j.rineng.2023.101744
10. Fountas N. A., Kostazos P., Pavlidis H., Antoniou V., Manolakos D. E., and Vaxevanidis N. M., Experimental investigation and statistical modelling for assessing the tensile properties of FDM fabricated parts. Procedia Structural Integrity, Vol. 26, 2020, pp. 139–146.
11. Wang P., Zou B., Ding S., Li L., and Huang C., Effects of FDM-3D printing parameters on mechanical properties and microstructure of CF/PEEK and GF/PEEK. Chinese Journal of Aeronautics, Vol. 34, No. 9, 2021, pp. 236–246. https://doi.org/10.1016/j.cja.2020.05.040
12. Hosseini S. S., Nabavi-Kivi A., Ayatollahi M. R., and Petru M., Effect of nozzle diameter on tensile and fracture behavior of FDM-PLA samples. Procedia Structural Integrity, Vol. 61, 2024, pp. 20–25.

https://doi.org/10.1111/ffe.14329
13. Pernet B., Nagel J. K., and Zhang H., Compressive Strength Assessment of 3D Printing Infill Patterns. Procedia CIRP, 2022. https://doi.org/10.1016/j.procir.2022.02.114
14. Guan R. and Smith D., Influence of Infill Parameters on the Tensile Mechanical Properties of 3D Printed Parts. Journal of Emerging Investigators, Vol. 2, July 2020. https://doi.org/10.59720/20-052
15. He Y., Shen M., Wang Q., Wang T., and Pei X., Effects of FDM parameters and annealing on the mechanical and tribological properties of PEEK. Composite Structures, Vol. 313, 2023, Article 116901. https://doi.org/10.1016/j.compstruct.2023.116901
16. ASTM D638–14, Standard test method for tensile properties of plastics. ASTM International, 2014.
17. Chacón, J. M., Caminero, M. Á., García-Plaza, E., & Núñez, P. J. Additive manufacturing of PLA structures using fused deposition modelling: Effect of process parameters on mechanical properties and their optimal selection. Materials & Design, Vol. 124, 2017, pp. 143–157. https://doi.org/10.1016/j.matdes.2017.03.065
18. Ngo, T. D., Kashani, A., Imbalzano, G., Nguyen, K. T. Q., & Hui, D. Additive manufacturing (3D printing): A review of materials, methods, applications and challenges. Composites Part B: Engineering, Vol. 143, (2018), pp. 172–196. https://doi.org/10.1016/j.compositesb.2018.02.012
19. Song, Y., Wang, H., & Li, L. Effect of infill density on mechanical properties of 3D printed parts using Fused Deposition Modeling. Materials Today Communications, Vol. 24, 2020, 101141.